ELSEVIER

Journal of Alloys and Compounds 280 (1998) 273–278

Journal of ALLOYS AND COMPOUNDS

Synthesis and magnetic properties of haematite with different particle morphologies

M. Sorescu[a,*], R.A. Brand[b], D. Mihaila-Tarabasanu[c], L. Diamandescu[c]

[a]*Duquesne University, Bayer School of Natural and Environmental Sciences, Physics Department, Pittsburgh, Pennsylvania 15282, USA*
[b]*Gerhart Mercator Universität, Laboratorium für Angewandte Physik, D-47048 Duisburg, Germany*
[c]*Institute of Atomic Physics, National Institute of Materials Physics, R-76900 Bucharest-Magurele, Romania*

Received 14 May 1998

Abstract

Haematite particles of four different morphologies (polyhedral, platelike, needlelike and diskshape) were synthesized by the hydrothermal method. The morphology and average particle diameter (1.4; 7.4; 0.2 and 0.12 μm, respectively) were determined by transmission electron microscopy (TEM) combined with electron diffraction. The haematite samples were studied by transmission Mössbauer spectroscopy in the temperature range 4.2–300 K. In all cases, a weak ferromagnetic phase (WF) was present above the Morin temperature of 230 K and found to coexist with an antiferromagnetic phase (AF) below this temperature. However, the populations of the two phases at 230 K were demonstrated to depend on the morphology of the particles. Moreover, the WF and AF phases exhibit a different dependence of the magnetic texture on temperature and particle morphology.

Keywords: Magnetic materials; Oxides; Chemical synthesis; Mössbauer spectroscopy; Magnetic properties

1. Introduction

The preparation and properties of iron oxides continue to attract considerable interest and attention because of their importance in magnetic materials technology. [1] In particular, it is known that the spin reorientations in haematite, α-Fe_2O_3, are determined to a large extent by the presence of impurities or substitutions and by the particle size [2–9].

The aim of this work is to present a detailed study of the role played by the particle morphology in determining the magnetic properties of haematite. For this purpose, haematite particles of four different morphologies (polyhedral, platelike, needlelike and diskshape) were synthesized by the hydrothermal method and studied by Mössbauer spectroscopy in the temperature range 4.2–300 K.

2. Experimental

The hydrothermal synthesis conditions (temperature, vapor pressure, time and filling factor of the autoclave) are summarized in Table 1. The morphology and average particle diameter $\langle \Phi \rangle$ were determined by TEM and electron diffraction. The corresponding micrographs are given in Fig. 1. Room and low temperature Mössbauer spectra were recorded with the γ rays perpendicular to the plane of the absorber using a constant acceleration spectrometer. The 25 mCi γ-ray source was ^{57}Co diffused in a Rh matrix. Least squares fitting of the Mössbauer spectra was performed with the NORMOS program [10].

3. Results and discussion

Transmission Mössbauer spectra of polyhedral, platelike, needlelike and diskshape haematite samples, recorded at 300, 230, 77 and 4.2 K are given in Figs. 2–5, respectively. The fitted values of the hyperfine parameters are listed in Tables 2–5 .

The room temperature Mössbauer spectra could be analyzed with one six-line Zeeman pattern, corresponding to the weak ferromagnetic phase [4]. It can be seen that the values of the hyperfine magnetic field and isomer shift are similar within the limits of experimental errors for the haematites of different morphologies. As expected, the hyperfine field of the weak ferromagnetic phase increases with decreasing temperature.

*Corresponding author. Tel.: +1412-396-4166 (office), +1412-396-5277 (lab); Fax: +1412-396-4829; E-mail: sorescu@duq3.cc.duq.edu

0925-8388/98/$ – see front matter
PII: S0925-8388(98)00719-1

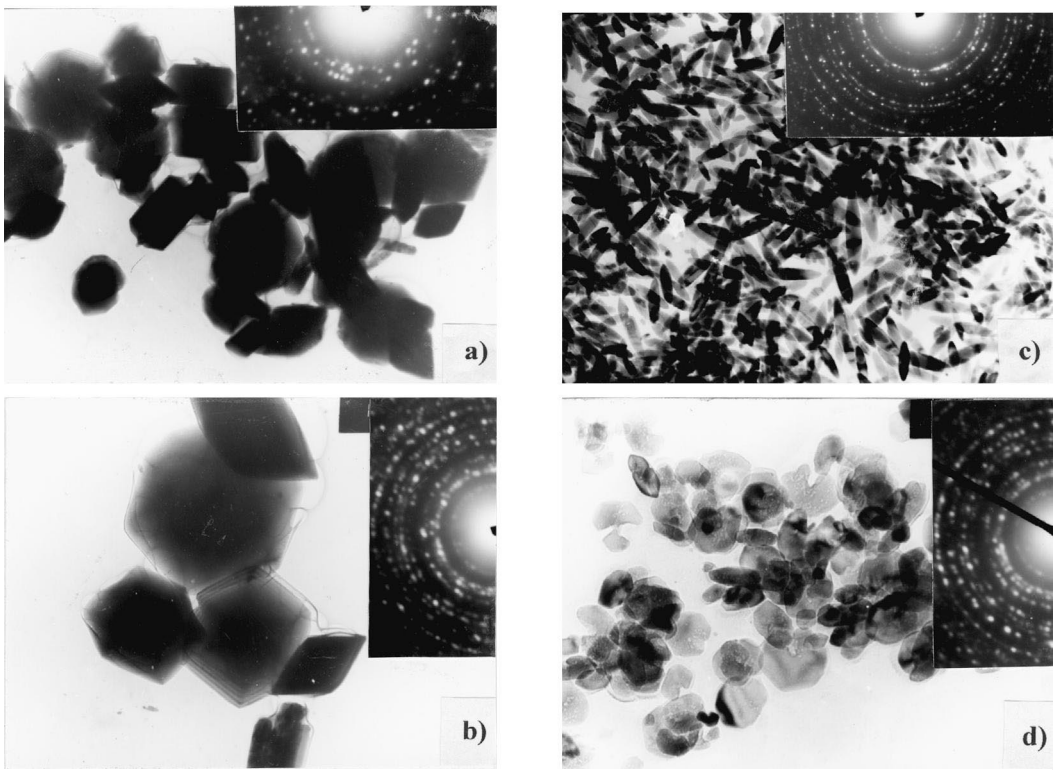

Fig. 1. Transmission electron microscopy and electron diffraction results for the haematite particles: (a) polyhedral; (b) platelike; (c) needlelike and (d) diskshape.

The Mössbauer spectra recorded at 230, 77 and 4.2 K were analyzed by considering two sextets, corresponding to the weak ferromagnetic and antiferromagnetic phases. The hyperfine magnetic field of the antiferromagnetic phase also increases with decreasing temperature. For all samples, the two phases were found to coexist, but in different proportions, depending on the morphology of the particles.

Fig. 6 shows the temperature dependence of the populations of the weak ferromagnetic phase as a function of temperature, for all morphologies investigated. In particular, it can be seen that for each morphology, the Morin temperature (defined as the temperature for which the antiferromagnetic phase is reduced to 50% of the value [4]) is different from the Morin temperature of 230 K, corresponding to bulk haematite. Thus, the Morin temperature is shifted to lower values for the polyhedral and platelike haematites, whereas the Morin temperature corresponding to needlelike and diskshape haematites is shifted to temperatures higher than 230 K. For all cases, the weak ferromagnetic phase represents 100% of the populations at room temperature. It should be noted, however, that the antiferromagnetic phase in diskshape haematite represents 99.2% of the population at liquid helium temperature. It may also be noted that the haematite of needlelike morphology is the only one exhibiting a nonmonotonic dependence on temperature of the population of the weak ferromagnetic phase.

Figs. 7 and 8 plot the temperature dependence of the magnetic texture parameter R_{21}, defined as the areal intensity ratio of the second to the first line, corresponding to the weak ferromagnetic and aniferromagnetic phases, respectively. It may be seen that each morphology is characterized by a different temperature dependence, with

Table 1
Hydrothermal parameters and dimensions (precursors, temperature T, pressure p_{vap}, time t, filling factor f and average particle diameter $\langle \Phi \rangle$) for the synthesis of haematite particles with different morphologies

Morphology	Precursors	T (K)	p_{vap} (atm)	t (h)	f	$\langle \Phi \rangle$ (μm)
polyhedral	α-FeOOH	473	7.0	2.0	0.55	1.40
platelike	$FeSO_4$/NaOH	473	16.0	2.0	0.55	7.40
needlelike	$FeCl_3$/NH_3	433	7.0	1.0	0.55	0.20
diskshape	$Fe(NO_3)_3$/KOH	393	2.0	3.5	0.54	0.12

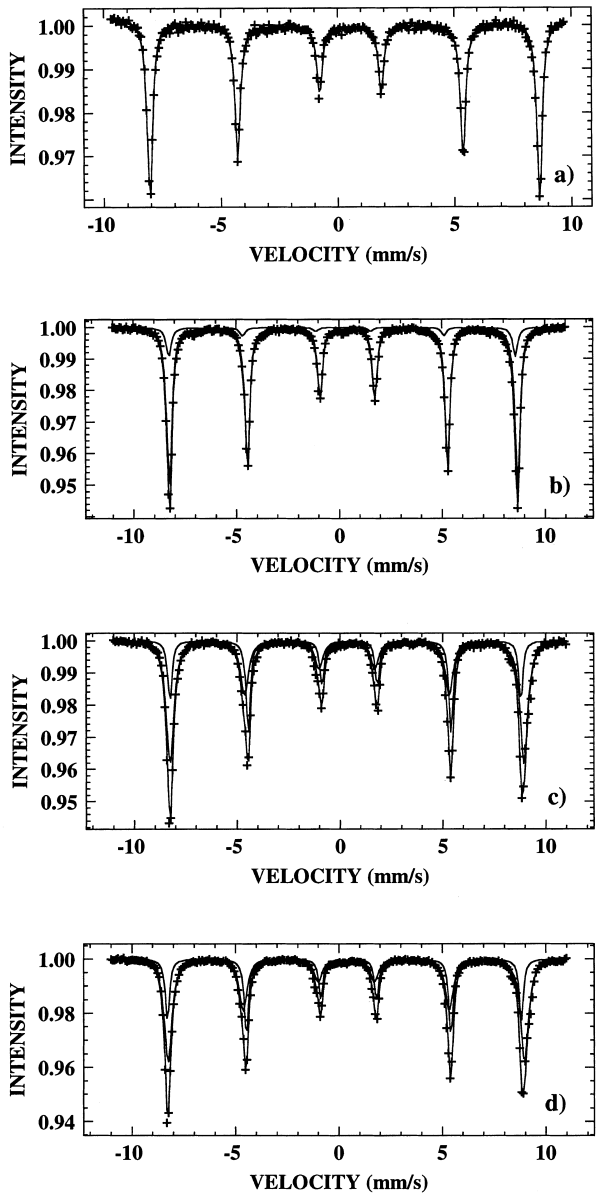

Fig. 2. Transmission Mössbauer spectra of the polyhedral haematite recorded at temperatures of: (a) 300 K; (b) 230 K; (c) 77 K and (d) 4.2 K.

a broad range of orientations existing at the Morin temperature. Again, the haematite with a needlelike morphology exhibits a nonmonotonic temperature dependence of the magnetic texture corresponding to the antiferromagnetic phase (Fig. 8).

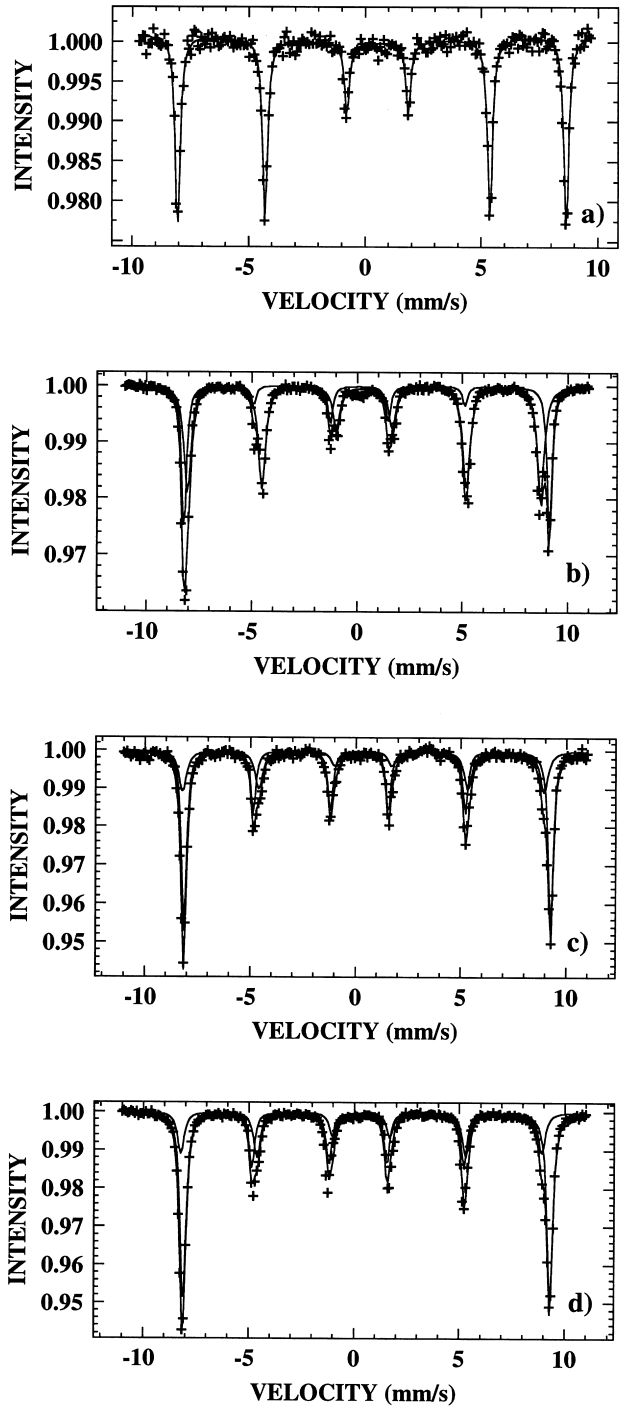

Fig. 3. Transmission Mössbauer spectra of the platelike haematite recorded at temperatures of: (a) 300 K; (b) 230 K; (c) 77 K and (d) 4.2 K.

4. Conclusions

This work reports on the hydrothermal synthesis and magnetic properties of haematite of four different particle morphologies: polyhedral, platelike, needlelike and diskshape. Mössbauer spectroscopy studies performed in the temperature range 4.2–300 K revealed the coexistence of the weak ferromagnetic and antiferromagnetic phases, in proportions depending on the particle morphology. Compared to the Morin temperature of bulk haematite, the Morin temperature of polyhedral and platelike haematites was found to shift to lower values, while the Morin temperature of needlelike and diskshape haematites was displaced to higher values. Moreover, the temperature

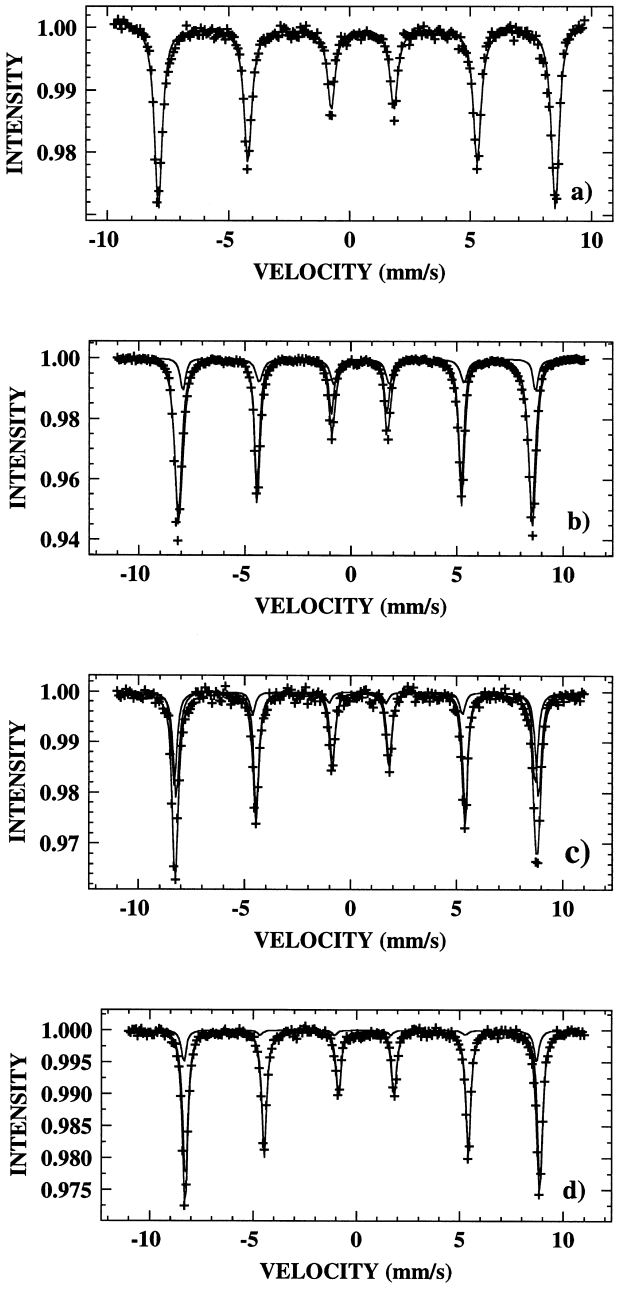

Fig. 4. Transmission Mössbauer spectra of the needlelike haematite recorded at temperatures of: (a) 300 K; (b) 230 K; (c) 77 K and (d) 4.2 K.

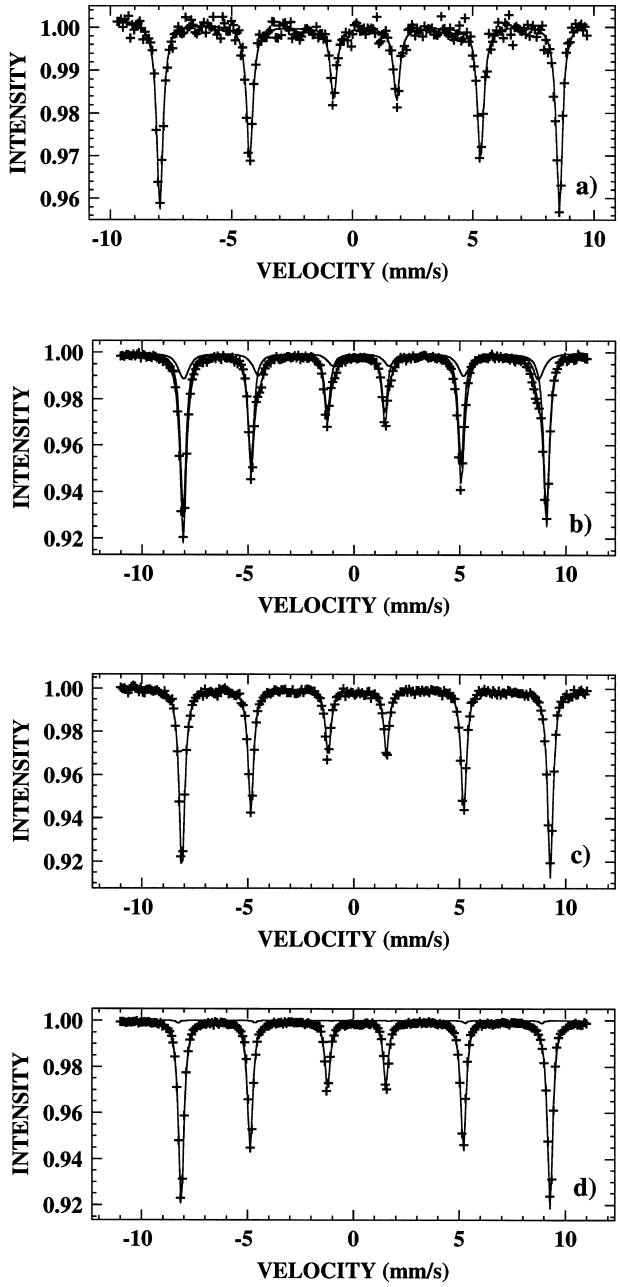

Fig. 5. Transmission Mössbauer spectra of the diskshape haematite recorded at temperatures of: (a) 300 K; (b) 230 K; (c) 77 K and (d) 4.2 K.

dependence of the magnetic texture parameter was found to be determined by the morphology involved, with a broad range of values at the Morin temperature.

Acknowledgements

This work was supported by a Cottrell College Science Award of Research Corporation.

Table 2
Hyperfine magnetic field H_{hf}, quadrupole shift 2ε, isomer shift δ (relative to α-Fe at 300 K), magnetic texture parameter R_{21} and relative areas corresponding to the component patterns in the transmission Mössbauer spectra of polyhedral α-Fe_2O_3

Morphology	T (K)	H_{hf} (T)	2ε (mm/s)	δ (mm/s)	R_{21}	Relative areas (%)	Assignment of sites
polyhedral	300	52.53	0.00	0.20	0.59	100.0	WF
	230	52.52	0.00	0.21	0.67	43.2	AF
		52.24	0.26	0.28	0.65	56.8	WF
	77	53.36	0.00	0.33	0.66	65.2	AF
		52.92	0.21	0.36	0.68	34.8	WF
	4.2	53.44	0.00	0.35	0.75	64.4	AF
		53.07	0.21	0.36	0.63	35.6	WF
Errors:	±0.1	±1.00	±0.05	±0.05	±0.05	±1.0	

Table 3
Hyperfine magnetic field H_{hf}, quadrupole shift 2ε, isomer shift δ (relative to α-Fe at 300 K), magnetic texture parameter R_{21} and relative areas corresponding to the component patterns in the transmission Mössbauer spectra of platelike α-Fe_2O_3

Morphology	T (K)	H_{hf} (T)	2ε (mm/s)	δ (mm/s)	R_{21}	Relative areas (%)	Assignment of sites
platelike	300	52.71	0.00	0.21	0.66	100.0	WF
	230	53.76	0.36	0.28	0.17	34.9	AF
		51.99	0.00	0.33	0.80	65.1	WF
	77	53.95	0.38	0.36	0.33	66.9	AF
		53.18	0.00	0.36	0.85	33.1	WF
	4.2	53.97	0.41	0.38	0.35	69.1	AF
		53.10	0.00	0.33	0.59	30.9	WF
Errors:	±0.1	±1.00	±0.05	±0.05	±0.05	±1.0	

Table 4
Hyperfine magnetic field H_{hf}, quadrupole shift 2ε, isomer shift δ (relative to α-Fe at 300 K), magnetic texture parameter R_{21} and relative areas corresponding to the component patterns in the transmission Mössbauer spectra of needlelike α-Fe_2O_3

Morphology	T (K)	H_{hf} (T)	2ε (mm/s)	δ (mm/s)	R_{21}	Relative areas (%)	Assignment of sites
needlelike	300	51.50	0.00	0.20	0.53	100.0	WF
	230	51.72	0.30	0.35	0.30	56.9	AF
		51.60	0.00	0.39	0.77	43.1	WF
	77	52.99	0.00	0.32	0.66	35.1	AF
		52.79	0.27	0.34	0.56	64.9	WF
	4.2	53.20	0.00	0.29	0.32	43.9	AF
		52.91	0.29	0.32	0.64	56.1	WF
Errors:	±0.1	±1.00	±0.05	±0.05	±0.05	±1.0	

Table 5
Hyperfine magnetic field H_{hf}, quadrupole shift 2ε, isomer shift δ (relative to α-Fe at 300 K), magnetic texture parameter R_{21} and relative areas corresponding to the component patterns in the transmission Mössbauer spectra of diskshape α-Fe_2O_3

Morphology	T (K)	H_{hf} (T)	2ε (mm/s)	δ (mm/s)	R_{21}	Relative areas (%)	Assignment of sites
diskshape	300	51.97	0.00	0.20	0.55	100.0	WF
	230	53.19	0.41	0.30	0.61	72.8	AF
		51.95	0.00	0.33	0.59	27.2	WF
	77	53.90	0.41	0.37	0.61	99.8	AF
		49.80	0.00	0.64	0.59	0.2	WF
	4.2	53.98	0.41	0.36	0.65	99.2	AF
		53.21	0.00	0.31	0.59	0.8	WF
Errors:	±0.1	±1.00	±0.05	±0.05	±0.05	±1.0	

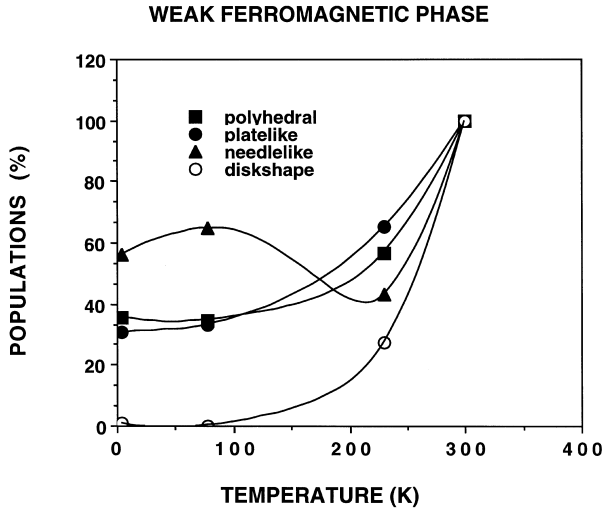

Fig. 6. The population of the weak ferromagnetic phase as a function of temperature, for haematite particles of different morphologies.

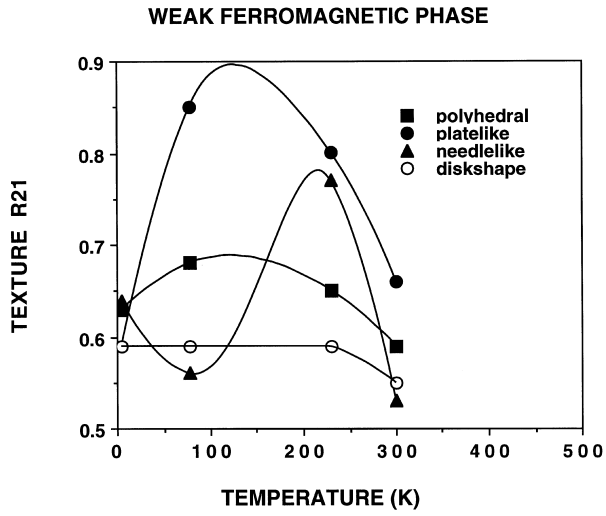

Fig. 7. The magnetic texture parameter of the weak ferromagnetic phase as a function of temperature, for haematite particles of different morphologies.

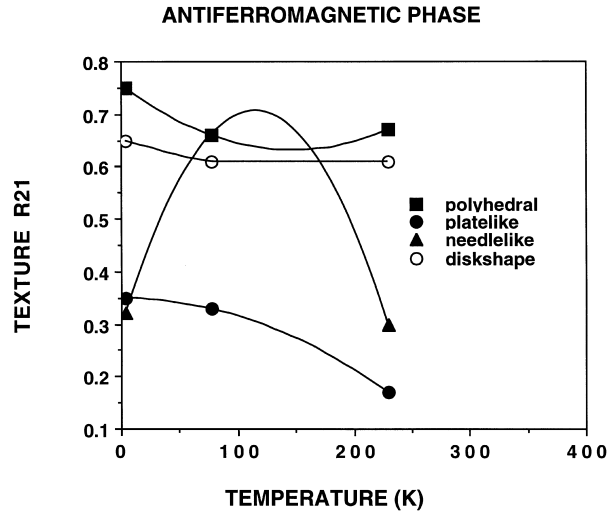

Fig. 8. The magnetic texture parameter of the antiferromagnetic phase as a function of temperature, for haematite particles of different morphologies.

References

[1] M. Sorescu, D. Mihaila–Tarabasanu, L. Diamandescu, Appl. Phys. Lett., 72 (1998) 2047.
[2] E. De Grave, D. Chambaere, L.H. Bowen, J. Magn. Magn. Mater. 30 (1983) 349.
[3] R.C. Nininger, D. Schroer, J. Phys. Chem. Solids 39 (1978) 137.
[4] A.E. Verbeeck, E. De Grave, R.E. Vandenberghe, Hyperfine Interact. 28 (1986) 639.
[5] H. Fei, M. Gao, X. Ai, Y. Yang, T. Zhang, J. Shen, Appl. Phys. A 62 (1996) 525.
[6] D.V. Dimitrov, G.C. Hadjipanayis, V. Papaefthymiou, A. Simopoulos, J. Vac. Sci. Technol. A 15 (1997) 1473.
[7] L. Jacyna-Onyszkiewicz, M. Grunwald-Wyspianska, W.A. Kaczmarek, J. Phys. IV FRANCE 7 (1997) 615.
[8] S.J. Campbell, W.A. Kaczmarek, G.M. Wang, NanoStructured Mater. 6 (1995) 735.
[9] I. Mitov, Z. Cherkezova-Zheleva, V. Mitrov, Phys. Status Solidi A: 161 (1997) 475.
[10] R.A. Brand, J. Lauer, D.M. Herlach, J. Phys. F 18 (1983) 675.